SUPPLEMENTARY MATERIALS

Photoelectrochemical Behavior of the Ternary Heterostructured Systems CdS/WO_3/TiO_2

A.A. Murashkina,[a] T.V. Bakiev,[a] Yu.M. Artemiev,[a] A.V. Rudakova,[a] A.V. Emeline,[a] and D.W. Bahnemann[a, b, *]

[a)] *Laboratory “Photoactive Nanocomposite Materials“, Saint-Petersburg State University, Ulyanovskaya Str. 1, Peterhof, Saint-Petersburg, 198504 Russia*

[b)] *Leibniz University of Hannover, Callinstrasse 3, Hannover 30167, Germany*

[*)] e-mail: bahnemann@iftc.uni-hannover.de

XRD data

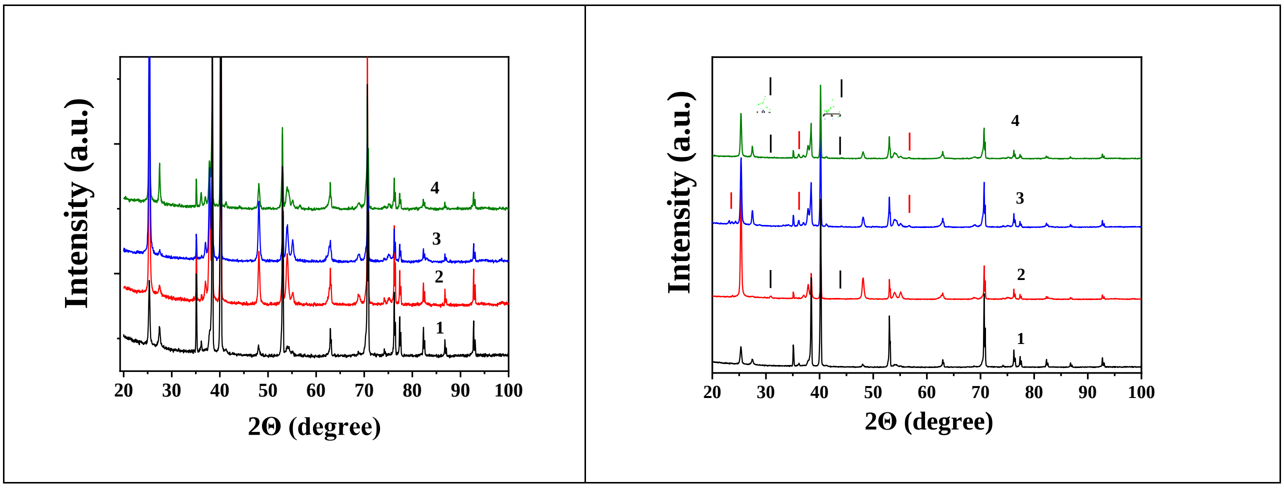

Figure S1. XRD patterns of planar samples: 1 - TiO_2, 2 – CdS/TiO_2, 3 - WO_3/TiO_2, 4 - WO_3/CdS/TiO_2 (left); nanotubes: 1 - TiO_2, 2 – CdS/TiO_2, 3 - WO_3/TiO_2, 4 - WO_3/CdS/TiO_2, Black lines show the replicas of CdS, red lines – WO_3

Electron microscopy

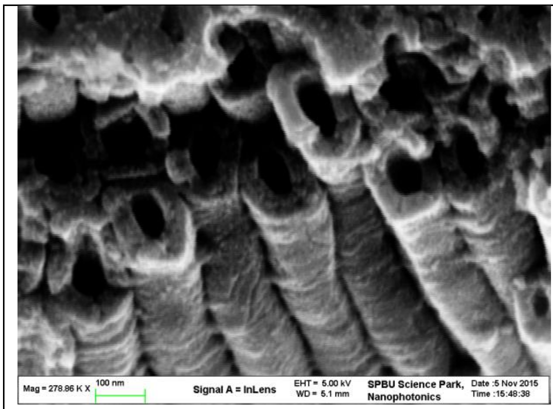

1)

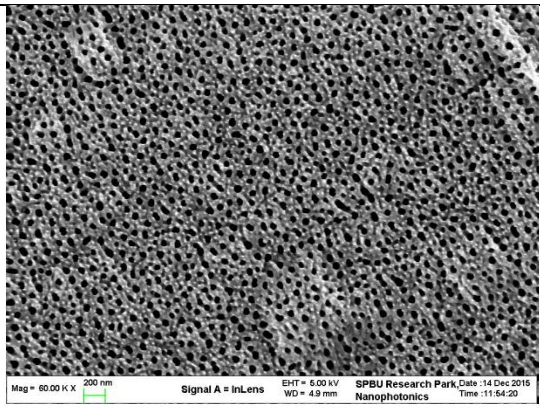

2)

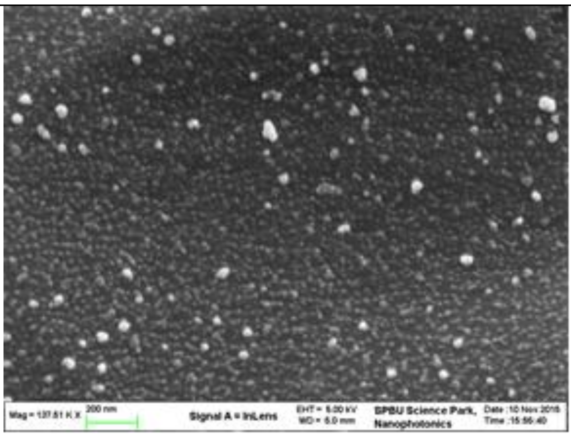
3)

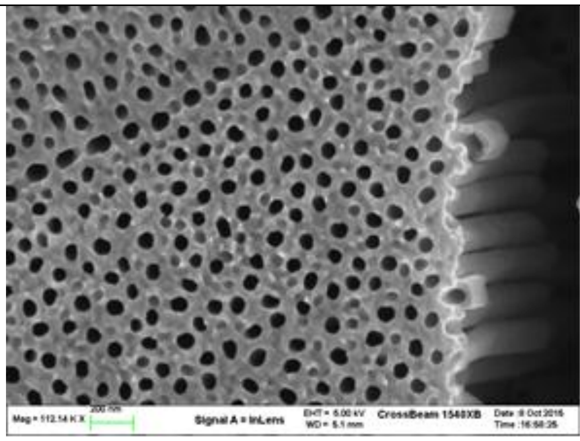
4)

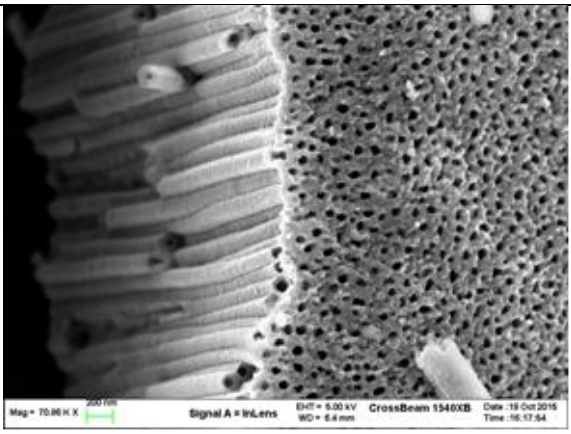
5)

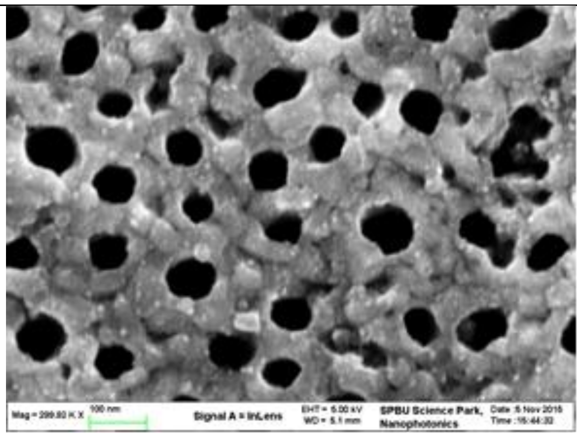
6)

Figure S2. SEM images of the titania nanotube (TNT) based systems: 1, 2 – TNTs (side and top view), 3 – tungsten metal particles deposited on Ti foil (before anodizing), 4 – TNTs/WO_3, 5 – CdS/TNTs, 6 – CdS/TNTs/WO_3.

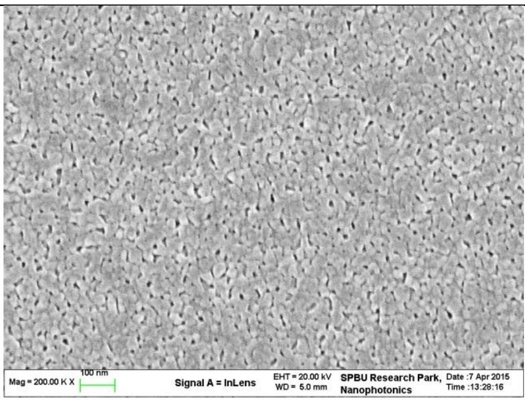
1

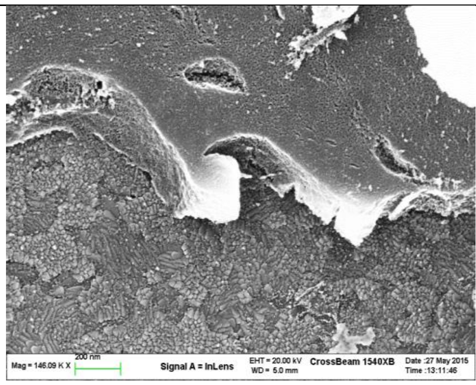
2

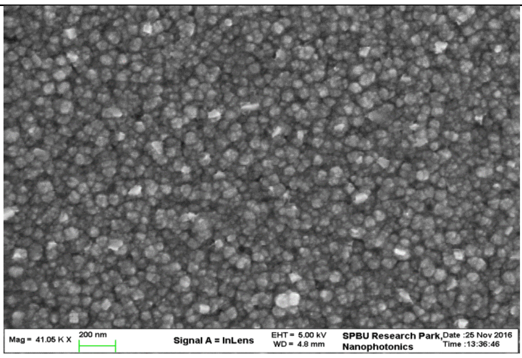
3

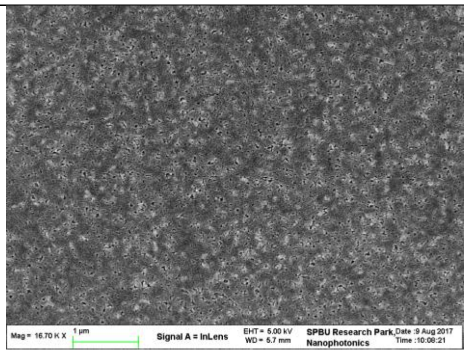
4

5

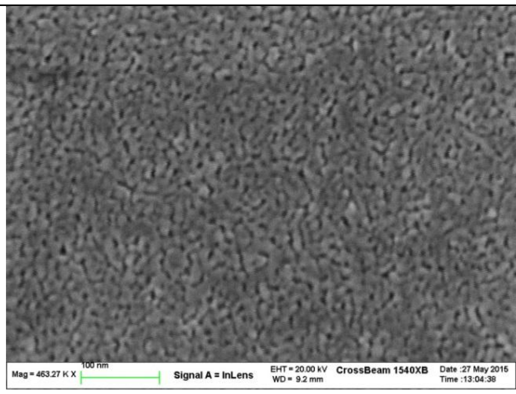

6

Figure S3. SEM images of planar systems on FTO glass substrates: 1 – TiO_2 (top view), 2 – $TiO_2/WO_3/CdS$ (side view), 3 – CdS (top view), 4 – TiO_2/CdS (top view), 5 – WO_3 (top view), 5 –TiO_2/WO_3 (top view).

XPS data

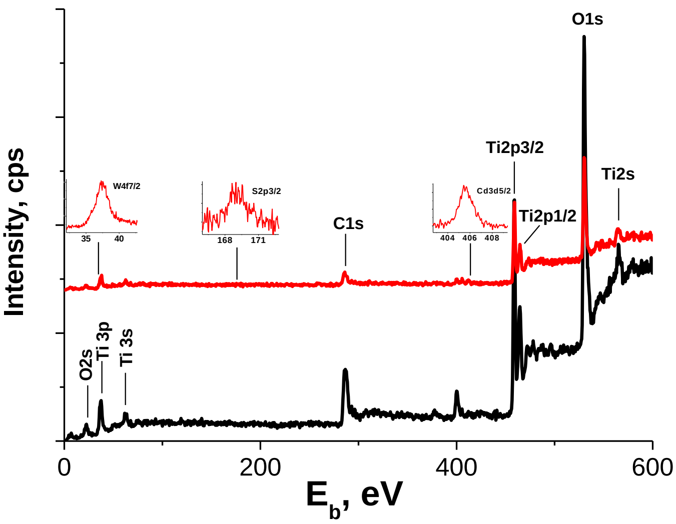

Figure S4. XPS spectra: TNT (black), CdS/WO_3 TNT (red).

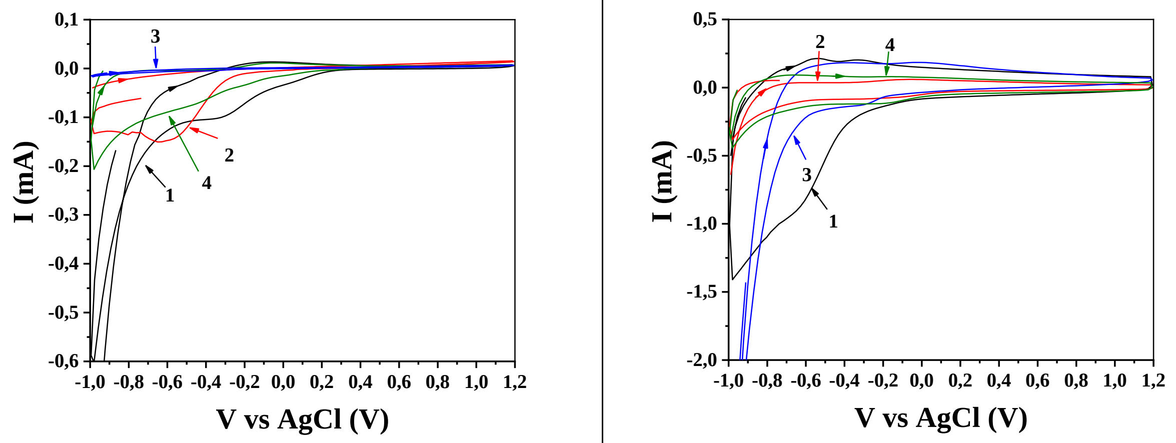

Figure S5. Linear sweep voltammetry (LSV) curves recorded under the dark conditions. Potential scan rate: 20 mV/s. Planar electrodes: 1 - TiO_2, 2 – CdS/TiO_2, 3 - WO_3/TiO_2, 4 - $WO_3/CdS/TiO_2$; (left); nanotube-based electrodes: 1 - TiO_2, 2 – CdS/TiO_2, 3 - WO_3/TiO_2, 4 - $WO_3/CdS/TiO_2$; (right).

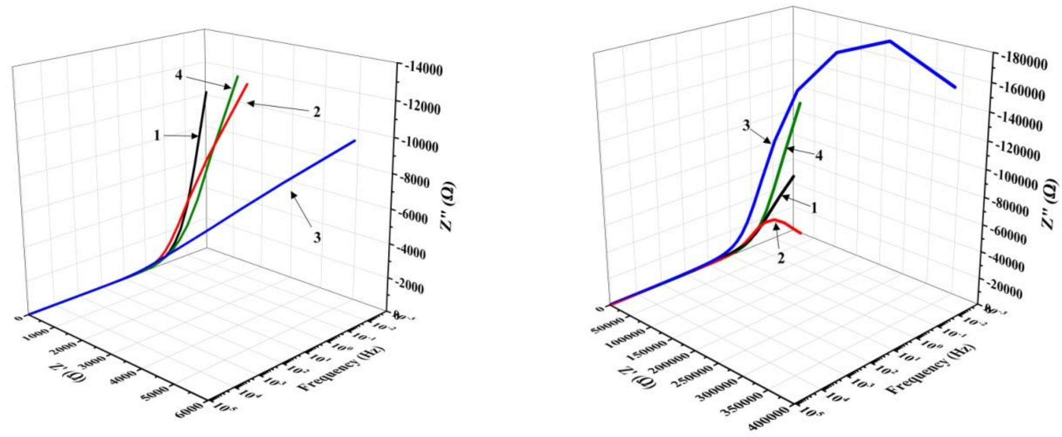

a) b)

Figure S6. 3D EIS plots recorded in the dark. a) nanotube-based electrodes: 1 - TiO_2, 2 – CdS/TiO_2, 3 - WO_3/TiO_2, 4 - $WO_3/CdS/TiO_2$; b) planar electrodes: 1 - TiO_2, 2 – CdS/TiO_2, 3 - WO_3/TiO_2, 4 – $CdS/WO_3/TiO_2$.

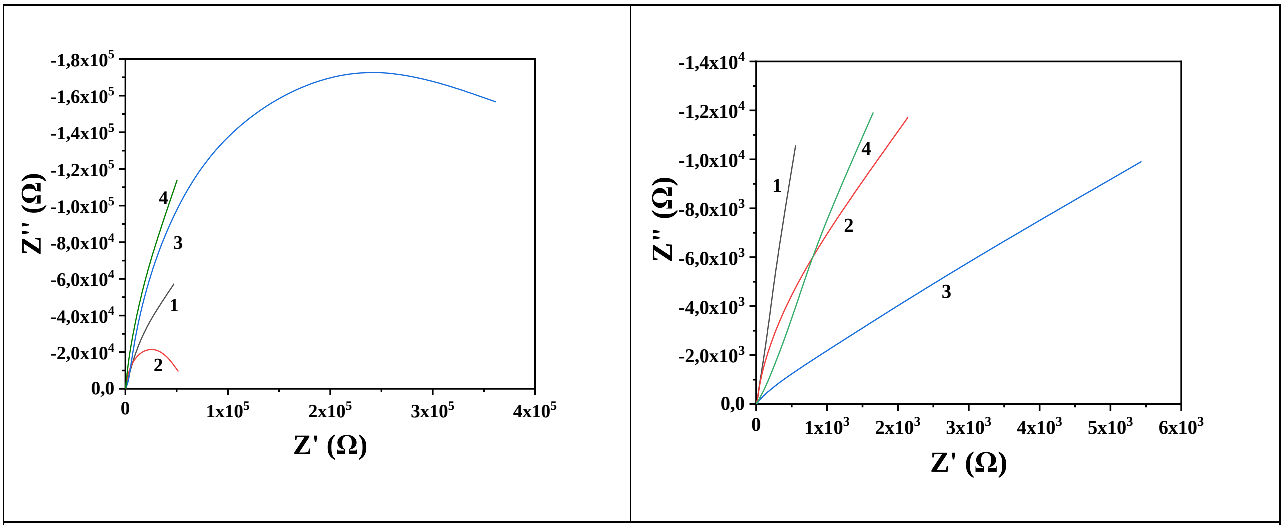

Figure S7. EIS Nyquist plots recorded in the dark. Samples: planar 1 - TiO_2, 2 – CdS/TiO_2, 3 - WO_3/TiO_2, 4 - $WO_3/CdS/TiO_2$ (left); nanotube-based 1 - TiO_2, 2 – CdS/TiO_2, 3 - WO_3/TiO_2, 4 - $WO_3/CdS/TiO_2$ (right).

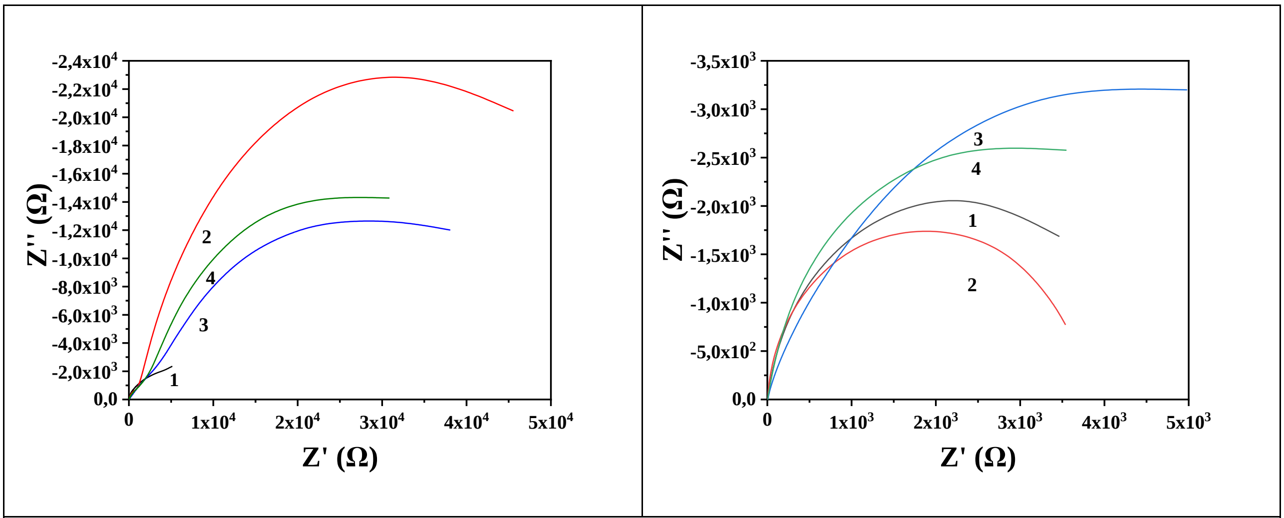

Figure S8. EIS Nyquist plots. Data recorded under illumination. Samples: planar 1 - TiO_2, 2 – CdS/TiO_2, 3 - WO_3/TiO_2, 4 - $WO_3/CdS/TiO_2$ (left); nanotube-based 1 - TiO_2, 2 – CdS/TiO_2, 3 - WO_3/TiO_2, 4 - $WO_3/CdS/TiO_2$ (right).

Table S1. Parameters of equivalent circuit scheme for nanotube-based systems in the dark.

Sample	R1, Ohm	R2, Ohm	P1	n1
TiO_2	~0	700000 ± 100000	0,0027 ± 0,0003	0,97 ± 0,01
CdS/TiO_2	~0	80000 ± 5000	0,00135 ± 0,00006	0,97 ± 0,01
WO_3/TiO_2	~0	80000 ± 5000	0,000714 ± 0,000004	0,75 ± 0,02
$CdS/WO_3/TiO_2$	~0	100000 ± 300000	0,00199 ± 0,000008	0,91 ± 0,01

Table S2.

dark	R1	R2	P1	n1
TiO2	30 ±80	176000 ±7000	0,000118 ±0,000001	0,79 ±0,01
CdSTiO2	200 ±100	49100 ±800	0,000103 ±0,00002	0,95 ±0,01
WO3TiO2	700 ±400	399000 ±8000	0,0000268 ±0000003	0,89 ±0,02
CdSWO3TiO2	70 ±30	380000 ±20000	0,000173 ±0,0000007	0,90 ±0,02

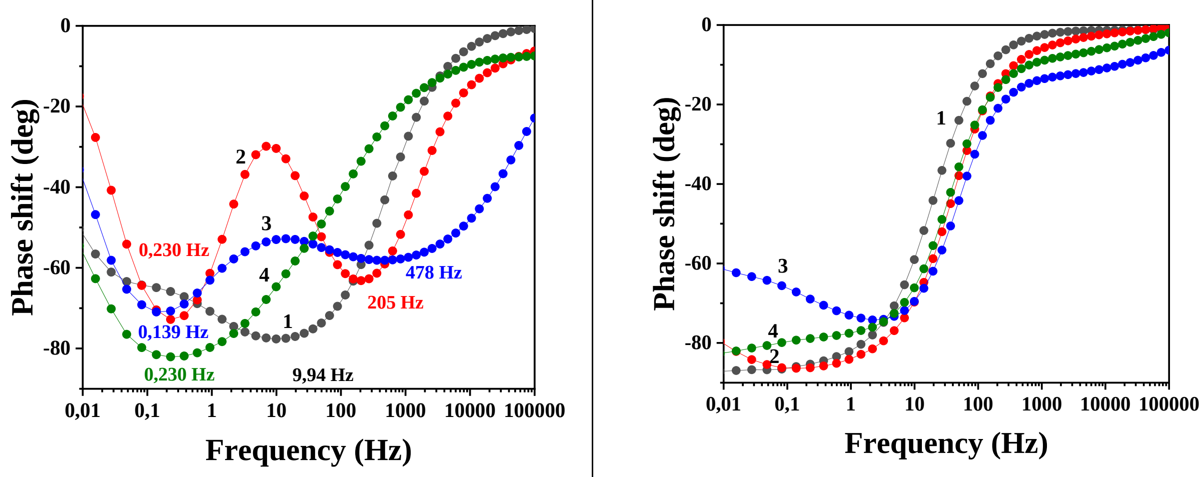

Figure S9. EIS Bode plots. Data recorded under dark conditions. Samples: planar 1 - TiO_2, 2 – CdS/TiO_2, 3 - WO_3/TiO_2, 4 - $WO_3/CdS/TiO_2$ (left); nanotube-based 1 - TiO_2, 2 – CdS/TiO_2, 3 - WO_3/TiO_2, 4 - $WO_3/CdS/TiO_2$ (right).

Table S3. The time constants τ calculated from Bode diagrams for nanotube heterostructures in the dark.

sample	frequency, Hz	τ, sec
TiO_2	0,00889	17,9
Cd_S/TiO_2	0,139	1,145
WO_3/TiO_2	2,19	0,0727
$CdS/WO_3/TiO_2$	0,00889	17,9

Table S4. The time constants τ calculated from Bode diagrams for planar heterostructures in the dark.

sample	frequency, Hz	t, sec
TiO_2	9,94	0,0160
CdS/TiO_2	0,23	0,692
CdS/TiO_2	205	0,000776
WO_3/TiO_2	0,139	1,145
WO_3/TiO_2	478	0,000333
$CdS/WO_3/TiO_2$	0,23	0,692